ISS Fly Around Strategy for Automated Docking of HTV-X

Moeko Hidaka, Naomi Murakami, Takahiro Sasaki,Yuki Tomita, Yuri Hachiya, Yoshinori Kondoh,
Takashi Uchiyama, Maki Maeda, Ryo Nakamura, Toru Yamamoto and Koji Yamanaka
Japan Aerospace Exploration Agency, 2-1-1 Sengen, Tsukuba-shi, Ibaraki, 305-8505 Japan

The Japan Aerospace Exploration Agency (JAXA) plans to demonstrate an automated docking technique with the next-generation visiting vehicle, the HTV-X, for future cis-lunar Gateway missions where crewed operation is not feasible. The docking demonstration will start after the HTV-X departs the ISS. The HTV-X then flies around to the zenith side of the ISS using Lidar navigation and approaches the ISS parallel to the R-bar for docking. This paper presents a GNC strategy, including the Lidar navigation algorithm for the fly-around phase. The safety of the proposed scenarios is demonstrated by numerical simulations.

HTV-X 自動ドッキングのための ISS 回り込みストラテジの検討

宇宙航空研究開発機構（JAXA）は，将来の Gateway ミッションに向けて，次世代補給機「HTV-X」による自動ドッキング技術の実証を計画している．ISS の離脱後，Lidar による航法値を使用して ISS の zenith 側にフライアラウンド，R-bar に沿って接近しドッキングする予定である．本論文では，フライアラウンドフェーズにおける Lidar 航法アルゴリズムを含む GNC ストラテジを紹介し，提案シナリオの安全性を数値シミュレーションにより示す.

I. Introduction

The Japan Aerospace Exploration Agency (JAXA) is developing a next-generation visiting vehicle, the HTV-X, to support the International Space Station (ISS) logistics for cargo transportation. Using the HTV-X, JAXA plans an additional mission of the automated docking technology with the ISS [1, 2]. The automated docking system is essential technology needed to realize sustainable activity on the future cis-lunar Gateway where crew-based operations such as capturing the rendezvous vehicle using a real-time robotic arm are not available.

Since the docking demonstration will start after a nominal berthing mission, the HTV-X's initial position is on the nadir side, released by the Space Station Robotic Manipulator System (SSRMS). In this demonstration, the International Docking Adapter (IDA) on the zenith side will be used, so the HTV-X flies around to the zenith side of the ISS using Lidar navigation. Next, it approaches the ISS parallel to the R-bar for docking.

This paper presents a GNC strategy, including the Lidar navigation algorithm for the fly-around phase. First, we show the candidates for fly-around scenarios and outline the trade-offs. Then, the GNC algorithms of the proposed scenario are described in detail. Since the ISS has many reflectors, it is necessary to consider the Lidar navigation algorithm that can be used when multiple reflectors are in the field of view. Finally, Monte Carlo (MC) simulations confirming the feasibility of the proposed scenarios are summarized. The ISS rendezvous requires a high level of safety; for example, the free-drift trajectory after maneuvers needs to be passively safe. Thus, the safety of the proposed scenario is also demonstrated.

II. Fly-Around Scenario Options

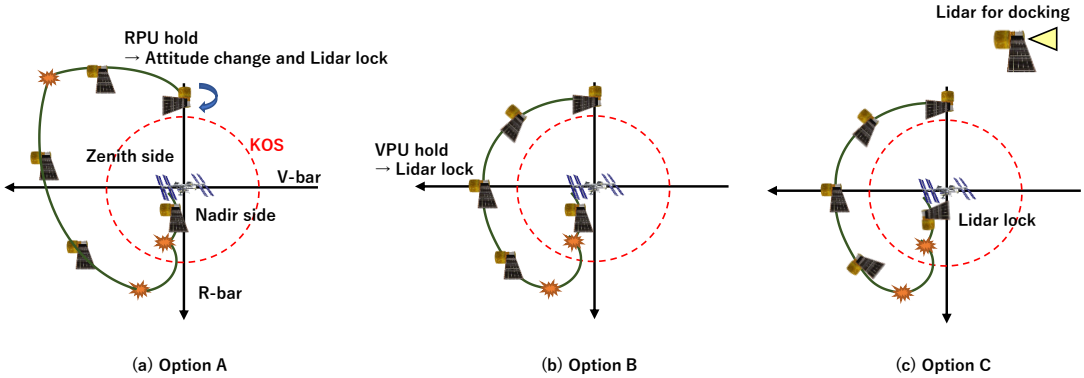

Fig. 1 Fly-Around Scenarios

Fig. 1 shows three options of fly-around scenarios. A faster and simpler fly-around scenario would be useful to respond to future operational demands such as port relocations, then this paper is limited to scenarios in which the HTV-X motion is constrained near the ISS. Because the operational range of the Lidar is short and the accuracy of the RGPS is not enough to control the HTV-X near the ISS, it is not easy to safely switch the navigation sensor from the RGPS to Lidar. For this reason, three options with different timing for switching to the Lidar navigation are studied.

In Option A, the HTV-X moves to the R-bar 300-meter point (RPU) using multiple impulse maneuvers employing the RGPS. This navigation method improves positioning accuracy by comparing GPS data acquired by HTV-X and the ISS. Conducting an RPU hold by impulse maneuvers, the HTV-X changes its attitude so that the Lidar points toward the ISS and switches from the RGPS to Lidar. However, at the RPU, the HTV-X moves significantly due to its altitude difference from the ISS. The HTV-X cannot stay within the Lidar operational range when held by the impulse maneuvers planned by the RGPS navigation, which is not accurate enough.

In Option B, the HTV-X moves to the V-bar 300-meter point (VPF) using multiple impulse maneuvers employing the RGPS. Conducting a VPF hold by impulse maneuvers, the vehicle switches the navigation sensor from the RGPS to Lidar. Then, controlling its attitude to point toward the ISS, the HTV-X moves to the RPU using the Lidar. From the VPF, the IDA of the zenith side to be docked is in the Lidar's field of view, so the HTV-X can track the same reflector until it docks. However, there is a risk of the HTV-X entering the ISS Keep Out Sphere (KOS) when the HTV-X uses the impulse maneuvers planned by the RGPS to stay at the VPF with a small altitude difference.

For Options A and B, switching the navigation sensor from the RGPS to Lidar is difficult after the HTV-X's departure. Then in Option C, the HTV-X departs with the Lidar locked on the reflector attached to the nadir side of the ISS. The HTV-X departs rotated 90° from its normal departure posture. After leaving the KOS, the HTV-X maintains its attitude toward the ISS and moves to the RPU using the Lidar. Since the IDM of the zenith side is not visible until near the V-bar, the HTV-X needs to move to switch the reflector being tracked. However, there are many reflectors on the ISS, and it is difficult to identify the reflector to be tracked from the multiple reflectors in the Lidar's field of view during the fly-around. This study proposes the Lidar navigation algorithm that uses the average position of the reflectors in its field of view as the navigation value without identifying each reflector.

III. GNC models

This section discusses the GNC models of Option C in detail.

A. Navigation

In this scenario, only Lidar is used for navigation—it measures the elevation (η), azimuth (φ), and range (r) for all reflectors in the field of view. The measurement model for each reflector h_i^L is described as follows. $\boldsymbol{r}^L = [x^L\ y^L\ z^L]^T$ is the reflector position in the Lidar coordinate system.

$$h_i^L = [\eta \quad \varphi \quad r]^T = \left[\sin^{-1}\frac{y^L}{\sqrt{\boldsymbol{r^L}^T \cdot \boldsymbol{r^L}}} \quad \tan^{-1}\frac{x^L}{z^L} \quad \sqrt{\boldsymbol{r}^{L^T} \cdot \boldsymbol{r}^L}\right] \tag{1}$$

Then, the HTV-X calculates its relative position, $\boldsymbol{r}^{LVLH}$ in ISS-LVLH frame from the Lidar's measurements. To calculate the ISS Center of Gravity (CoG), which is the origin of the ISS- LVLH coordinate system, each reflector position relative to the ISS CoG needs to be known. Therefore each target needs to be identified. However, it is difficult to identify reflectors in the Lidar's field of view within a limited processing time. This is why the average position of all reflectors in the Lidar's field of view is used as the ISS CoG without identifying them.

$$\boldsymbol{r}^{LVLH} = [x^{LVLH} \quad y^{LVLH} \quad z^{LVLH}]^T = -\frac{1}{n}\sum_{i=1}^{n} \boldsymbol{C}_L^{LVLH}[x_i^L \quad y_i^L \quad z_i^L]^T + \boldsymbol{r}_{offset} \tag{2}$$

$\boldsymbol{C}_L^{LVLH}$ is the transition matrix from the Lidar coordinate system to the ISS-LVLH coordinate system, and $\boldsymbol{r}^L$ is calculated from the Lidar measurements as shown in Eq. (1). $\boldsymbol{r}_{offset}$ is the offset of the reflector positions from the ISS CoG, which is rough but can be analyzed in advance, and this is a constant value. Relative velocity in the ISS-LVLH coordinate system is calculated from the difference between the relative positions in the previous step.

A low-pass filter is applied for both relative position and velocity; α is set to 0.1.

$$\hat{\boldsymbol{r}}^{LVLH}(t) = \alpha \boldsymbol{r}^{LVLH}(t_k) + (1-\alpha)\hat{\boldsymbol{r}}^{LVLH}(t_{k-1}) \tag{3}$$

B. Attitude Control

The HTV-X departs rotated 90º from its normal departure posture. After leaving the KOS, the HTV-X's attitude is controlled so that the Lidar points toward the ISS center of gravity. Attitude control is performed using PD control, and input value $\Delta\boldsymbol{Tr}$ is calculated as follows.

$$\Delta\boldsymbol{Tr} = -\boldsymbol{K_p}\Delta\boldsymbol{\theta} - \boldsymbol{K_d}(\hat{\boldsymbol{\omega}} - \boldsymbol{\omega_d}) \tag{4}$$

$\Delta\boldsymbol{\theta}$ is the attitude error from the target values. $\boldsymbol{\omega}_d$ is the target angular velocity, and $\hat{\boldsymbol{\omega}}$ is the HTV-X's estimated angular velocity. The control gain is decided by trial and error. The quaternions and angular velocity of the HTV-X are estimated using an Extended Kalman Filter (EKF) based on the star tracker and gyro. The target values are calculated based on the ISS center of gravity, estimated from the Lidar navigation.

C. Orbital Control

After separation from ISS, the HTV-X executes ISS Departure Maneuver1 (IDM1), and IDM2 burns to get out of the KOS. After IDM2, the HTV-X performs the Fly-Around Maneuver (FAM), a pre-planned impulse maneuver, and starts PD control to approach RPU immediately after FAM. The input value for PD control is calculated as follows.

$$\Delta\boldsymbol{v}^{\boldsymbol{LVLH}} = -\boldsymbol{K_p}(\hat{\boldsymbol{r}} - \boldsymbol{r_d}) - \boldsymbol{K_d}(\hat{\boldsymbol{v}} - \boldsymbol{v_d}) \tag{5}$$

$\hat{\boldsymbol{r}}$, $\hat{\boldsymbol{v}}$ are HTV-X's estimated position and velocity based on the Lidar navigation. $\boldsymbol{r}_d, \boldsymbol{v}_d$ are position and velocity of the reference trajectory to be followed by PD control, as shown in Fig. 2. The reference trajectory is designed differently for FA1 and FA2. In the FA1 phase, the reference trajectory is a free-drift trajectory after FAM. As shown in Fig. 3, on the nadir side of the ISS, the HTV-X's free-drift trajectory is passive safety, flowing forward of the ISS. On the zenith side of the ISS, the HTV-X's free-drift trajectory is passive safety, flowing backward of the ISS. Therefore, when flying around from the nadir side to the zenith side, there is a time when the free-drift trajectory switches, and there is a risk of entering the KOS. If there is a risk of entering the KOS, it is necessary to design an active Collision Avoidance Maneuver (CAM), but it is important to minimize its duration. The FAM is a passive safe maneuver after which the free-drift trajectory flows backward of the ISS as long as it does not under-burn. Therefore, the PD control during the FA1 phase after the FAM only corrects the position errors caused by navigation errors, and the trajectory becomes passively safe even when control stops midway.

In the FA2 phase, the reference trajectory is an arc with a radius of 300 m centered on the ISS. The target velocity is a constant value in the first half of the FA2 phase and is calculated to decelerate linearly in the second half to zero at the RPU.

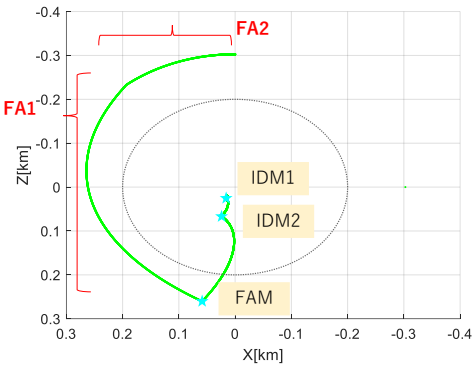

Fig. 2 Reference trajectory in ISS-LVLH frame

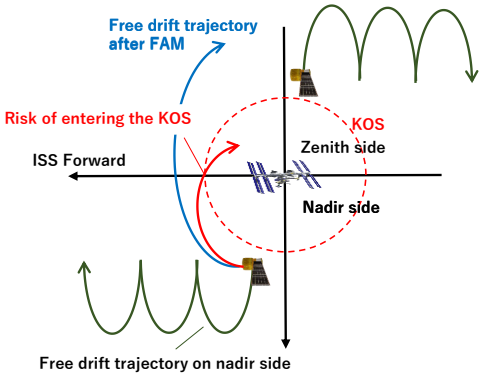

Fig. 3 Free-drift trajectory in ISS-LVLH frame

IV. Results

The validity of the proposed scenarios is demonstrated through numerical simulations. Table 1 shows simulation conditions. The misalignment is added as bias errors.

Table 1 Simulation conditions

Navigation filter	Position: Low-pass filter 2 Hz Attitude: Extended Kalman filter 2 Hz
PD control	Attitude control frequency: 2 Hz Orbital control frequency: 2 Hz
Lidar	Frequency: 2 Hz Operational range: 400 m Observation error: Azimuth/Elevation direction: 0.06º (3σ) Range direction: 0.3 % (3σ) Misalignment: 0.1º/axis
Star tracker	Frequency: 2 Hz Observation error: Optical axis direction: 122 arcsec (3σ) Orthogonal direction: 18 arcsec (3σ) Misalignment: 0.25º/axis
Gyro	ARW: 0.036º/√h (3σ) RRW: 10.25º/h/√h (3σ) Misalignment: 0º/axis
Maneuver	Impulse model Magnitude error: 3 %/axis (3σ)
Propagator	Gravity field: 20×20 harmonic model Relative atmospheric drag: 0 - 1.015 e-5 m/s^2 (Assign to each MC case as uniform distribution)

Fig. 4 shows the result of the fly-around scenario. The gray lines show the result of MC analysis of 300 cases, and nominal trajectory means that the random and bias errors are set to zero. For all MC cases, the HTV-X moves up to RPU, and the validity of the scenarios is shown.

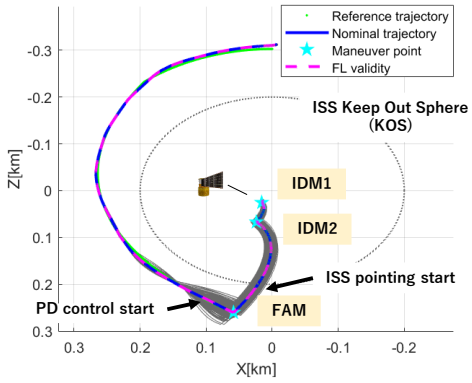

Fig. 4 Fly-around results in ISS-LVLH frame

Table 2 summarizes the execution time, guidance law, navigation type, and Δv of each burn. In the nominal case, the total Δv required from the ISS separation to the RPU arrival is 4.24 m/sec with a low-pass filter, and the total operation time is 3079 seconds.

Table 2 Burn list

Point	Time [s]	Guidance Law	Navigation	Δv [m/s]
IDM1	380	Planned	-	0.04
IDM2	979	Planned	-	0.20
FAM	1679	Planned	-	0.89
- RPU	1679	PD control	Lidar	2.90
RPU Hold	2979	PD control	Lidar	0.21

A. The Lidar Visibility

Even with the rough Lidar navigation using the average position of all reflectors in the field of view, the FL never loses the reflectors during the fly-around in the MC 300 cases. Fig. 5 shows the switching of the reflectors in the Lidar's field of view in the nominal case, and more than 20 reflector switches occurred.

Fig. 6 shows the orbit control input history during the fly-around in the nominal case. In this simulation, the maneuver is performed using an impulse model, so the amount of Δv per control frequency is limited during PD control. When the reflectors in the field of view are switched, the average position changes instantly. This causes a jump in the Lidar navigation value that the low-pass filter cannot completely remove, and the control input increases instantaneously.

B. Safety Analysis

Whether the free-drift trajectory is passively safe if control stops in the middle of the fly-around is checked in the safety analysis. At the beginning of the PD control, the control input to correct the FAM position becomes large, and the free-drift trajectory is not passively safe. However, it is passively safe after that, as shown in Fig. 7. The period when the active CAM design is necessary is reduced sufficiently.

Active CAM is required from the start of FAM until 100 seconds after the start of PD control. By switching acceleration and deceleration of the active CAM depending on the executed Δv of the FAM, the amount of Δv of the active CAM can be reduced. The design of the active CAM using Linear Covariance Analysis (LCA) [3, 4] shows that it is efficient to switch the acceleration and deceleration when 50 % of the FAM is executed, and the required Δv of the active CAM is 0.15 m/s (Fig. 8).

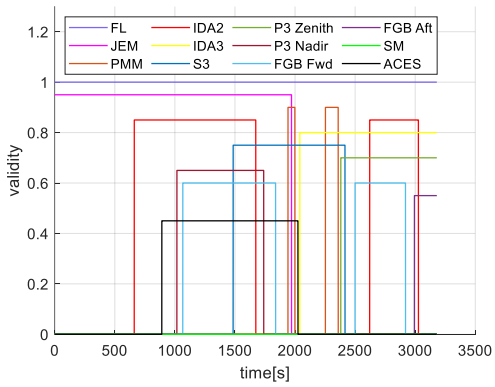

Fig. 5 Refractors switching in the nominal case

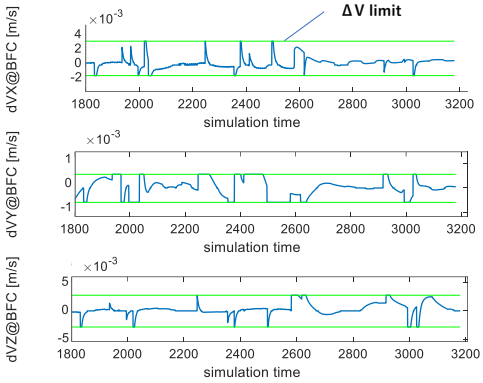

Fig. 6 Orbit control input in the nominal case

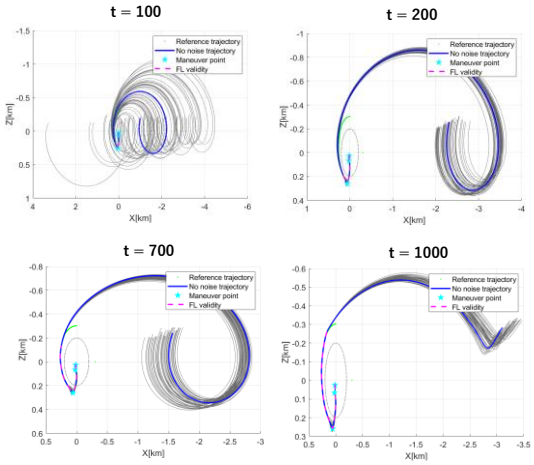

Fig. 7 Free-drift trajectory safety analysis

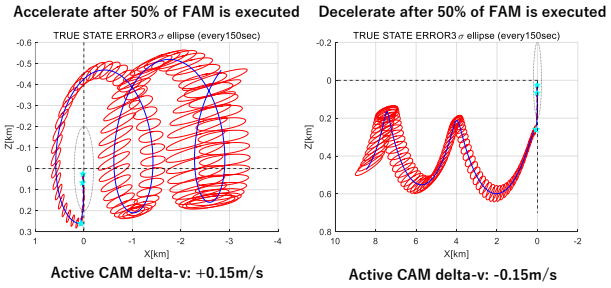

Fig. 8 Active CAM design (LCA)

V. Conclusion

In this study, several fly-around scenario options were presented for the HTV-X's automated docking demonstration. Then, the scenario that the authors are considering is described in detail and validated by numerical simulations. Using the average position of all reflectors in the Lidar's field of view, the HTV-X can fly around to the zenith port. However, since the control input becomes significant when the reflector switches, we would like to tune the control gain and consider a navigation filter.

References

[1] Y. Tomita, et al., "Development of Guidance, Navigation, and Control Strategy for the Automated Docking Operation on HTV-X," 71st International Astronautical Congress (IAC), The CyberSpace Edition, 12-14 October 2020.

[2] T. Sasaki, et al., "Proximity Operation and Guidance Navigation and Control Design for HTV-X Automated Docking Demonstration Mission," 31stWorkshop on JAXA Astrodynamics and Flight Mechanics, 2021.

[3] D. K. Geller, "Linear Covariance Techniques for Orbital Rendezvous Analysis and Autonomous Onboard Mission Planning," Journal of Guidance, Control, and Dynamics, Vol. 29, No. 6, 2006, pp. 1404–1414.

[4] D. K. Geller, M. B. Rose and D. C.Woffinden, "Event Triggers in Linear Covariance Analysis with Applications to Orbital Rendezvous," Journal of Guidance, Control, and Dynamics, vol. 32, no. 1, pp. 102-111, 2009.